PHYSICAL REVIEW A **78**, 062314 (2008)

Computation with coherent states via teleportations to and from a quantum bus

Marcus Silva[1,*] and Casey R. Myers[2,1,†]
[1]*Department of Physics and Astronomy, and Institute for Quantum Computing, University of Waterloo, ON, Canada N2L 3G1*
[2]*National Institute of Informatics, 2-1-2 Hitotsubashi, Chiyoda-ku, Tokyo 101-8430, Japan*

(Received 3 May 2008; revised manuscript received 26 September 2008; published 5 December 2008)

In this paper, we present results illustrating the power and flexibility of one-bit teleportations in quantum bus computation. We first show a scheme to perform a universal set of gates on continuous variable modes, which we call a quantum bus or *qubus*, using controlled phase-space rotations, homodyne detection, ancilla qubits, and single-qubit measurement. Within our comparison criteria, the resource usage for this scheme is lower than any previous scheme to date. We then illustrate how one-bit teleportations into a qubus can be used to encode qubit states into a quantum repetition code, which in turn can be used as an efficient method for producing Greenberger-Horne-Zeilinger states that can be used to create large cluster states. Each of these schemes can be modified so that teleportation measurements are post-selected to yield outputs with higher fidelity without changing the physical parameters of the system.

DOI: 10.1103/PhysRevA.78.062314 PACS number(s): 03.67.Lx, 03.67.Mn, 42.65.−k

I. INTRODUCTION

Bennett *et al.* [1] showed that an unknown quantum state (a qubit) could be *teleported* via two classical bits with the use of a maximally entangled Bell state shared between the sender and receiver. The significance of teleportation as a tool for quantum information was extended when Gottesman and Chuang [2] showed that unitary gates could be performed using modified teleportation protocols, known as *gate teleportation*, where the task of applying a certain gate was effectively translated to the task of preparing a certain state. Since then, teleportation has been an invaluable tool for the quantum-information community, as gate teleportation was the basis for showing that linear optics with single photons and photodetectors was sufficient for a scalable quantum computer [3]. Moreover, Zhou *et al.* [4] demonstrated that all previously known fault-tolerant gate constructions were equivalent to *one-bit teleportations* of gates.

Recently, the use of one-bit teleportations between a qubit and a continuous variable *quantum bus* (or *qubus*) has been shown to be important for fault tolerance [5]. Using one-bit teleportations to transfer between two different forms of quantum logic, a fault-tolerant method to measure the syndromes for any stabilizer code with the qubus architecture was shown, allowing for a linear saving in resources compared to a general controlled-NOT (CNOT) construction. In terms of optics, the two different types of quantum logic used were polarization $\{|0\rangle=|H\rangle,|1\rangle=|V\rangle\}$ and logical states corresponding to rotated coherent states $\{|\alpha\rangle,|e^{\pm i\theta}\alpha\rangle\}$, although in general any two-level system (qubit) that can interact with a continuous variable mode (qubus) would suffice. The relative ease with which single-qubit operations can be generally performed prompted the question of whether a universal set of gates can be constructed with this rotated coherent state logic. In this paper, we describe one such construction, which we call *qubus logic*.

The fault-tolerant error-correction scheme using a qubus [5] exploits the fact that entanglement is easy to create with coherent cat states of the qubus, such as $|\alpha\rangle+|\alpha e^{i\theta}\rangle$, and single-qubit operations are easily performed on a two-level system. In this paper, we describe how these cat sates can be used as a resource to construct other large entangled states, such as cluster states [6–8], using one-bit teleportations between a qubit and a qubus.

Although the average fidelities of qubus logic and cluster state preparation are dependent on how strong the interaction between the qubit and the qubus can be made, and how large the amplitude α is, these fidelities can be increased arbitrarily close to 1 through the use of post-selection during the one-bit teleportations, demonstrating the power and flexibility of teleportation in qubus computation for state preparation.

The paper is organized as follows. First, in Sec. II we revisit one-bit teleportations for the qubus scheme. Next, in Sec. III we present a technique to perform quantum computation using coherent states of the qubus as basis states. To do this, we make use of controlled (phase-space) rotations and ancilla qubits. This coherent state computation scheme is the most efficient to date. In Sec. IV, we show how we can efficiently prepare repetition encoded states using one-bit teleportations, and how such encoders can be used to prepare large cluster states.

II. ONE-BIT TELEPORTATIONS

In the original quantum teleportation protocol, an arbitrary quantum state can be transferred between two parties that share a maximally entangled state by using only measurements and communication of measurement outcomes [1]. Modifications of the resource state allow for the applications of unitaries to an arbitrary state in a similar manner, in what is known as *gate teleportation* [2]. The main advantage of gate teleportation is the fact that it allows for the application of the unitary to be delegated to the state preparation stage. In some physical realizations of quantum devices, it may only be possible to prepare these states with

*msilva@iqc.ca
†crmyers@nii.ac.jp

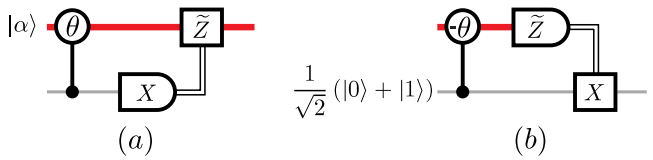

FIG. 1. (Color online) Approximate one-bit teleportation protocols [4] using controlled rotations. Here, the light gray lines correspond to qubits, and the thick red lines correspond to quantum bus modes.

some probability of success. In that case, the successful preparations can still be used for scalable quantum computation [2]. When dealing with noisy quantum devices, it is important to encode the quantum state across multiple subsystems, at the cost of requiring more complex operations to implement encoded unitaries. In order to avoid the uncontrolled propagation of errors during these operations, one can also employ gate teleportation with the extra step of verifying the integrity of the resource state before use [2–4,9,10]. In the cases in which the teleportation protocol is used only to separate the preparation of complex resource states from the rest of the computation, simpler protocols can be devised. These protocols are known as *one-bit teleportations* [4]. Unitaries implemented through one-bit gate teleportation can also be used for fault-tolerant quantum computation [4] as well as measurement-based quantum computation [6]. The main difference between one-bit teleportation and the standard teleportation protocol is the lack of a maximally entangled state. Instead, in order to perform a one-bit teleportation, it is necessary that the two parties interact directly in a specified manner, and that the qubit which will receive the teleported state be prepared in a special state initially.

Some unitary operations on coherent states can be difficult to implement deterministically, while the creation of entangled multimode coherent states is relatively easy. Single qubits, on the other hand, are usually relatively easy to manipulate, while interactions between them can be challenging. For this reason, we consider one-bit teleportation between states of a qubit and states of a field in a quantum bus, or *qubus*. The two types of one-bit teleportations for qubus computation are shown in Fig. 1, based on similar constructions proposed for qubits by Zhou *et al.* [4].

The one-bit teleportation of the qubit state $a|0\rangle+b|1\rangle$ into the state of the qubus, in the coherent state basis $\{|\alpha\rangle,|\alpha e^{i\theta}\rangle\}$, is depicted in Fig. 1(a). The qubit itself can be encoded, for example, in the polarization of a photon, i.e., $|0\rangle=|H\rangle$ and $|1\rangle=|V\rangle$. The initial state, before any operation, is $(a|0\rangle+b|1\rangle)|\alpha\rangle$. The controlled phase-space rotation corresponds to the unitary that applies a phase shift of θ to the bus if the qubit state is $|1\rangle$, and does nothing otherwise. Physically, this corresponds to the interaction Hamiltonian $\hat{H}_{\rm int}=-\hbar\chi\hat{a}^{\dagger}\hat{a}\hat{\Lambda}$ [11] between the bus and qubit, where $\theta=-\chi t$. This interaction could be a cross Kerr nonlinearity with $\hat{\Lambda}=\hat{b}^{\dagger}\hat{b}$, possibly implemented with electromagnetically induced transparency (EIT) [12,13] or a Jaynes-Cummings interaction in the dispersive limit with $\hat{\Lambda}=\hat{\sigma}_Z$, possibly implemented with cavity QED [14–16]. After the controlled rotation by θ, the state becomes $a|0\rangle|\alpha\rangle+b|1\rangle|e^{i\theta}\alpha\rangle$. Representing the qubit state in the Pauli X eigenbasis, this is $|+\rangle(a|\alpha\rangle+b|e^{i\theta}\alpha\rangle)/\sqrt{2}+|-\rangle(a|\alpha\rangle-b|e^{i\theta}\alpha\rangle)/\sqrt{2}$. When we detect $|+\rangle$, we have successfully teleported our qubit into $|\alpha\rangle$, $|e^{i\theta}\alpha\rangle$ logic. When we detect $|-\rangle$, we have the state $a|\alpha\rangle-b|e^{i\theta}\alpha\rangle$. The relative phase discrepancy can be corrected by the operation $\tilde{Z}$, which approximates the Pauli Z operation in the $\{|\alpha\rangle,|\alpha e^{i\theta}\rangle\}$ basis. This correction can be delayed until the state is teleported back to a qubit, where it is more easily implemented.

The one-bit teleportation of the state $a|\alpha\rangle+b|\alpha e^{i\theta}\rangle$ of the qubus to the state of the qubit can be performed by the circuit depicted in Fig. 1(b). That is, we start with the state $(a|\alpha\rangle+b|\alpha e^{i\theta}\rangle)(|0\rangle+|1\rangle)/\sqrt{2}$. After the controlled rotation by $-\theta$, the state becomes $|\alpha\rangle(a|0\rangle+b|1\rangle)/\sqrt{2}+(b|e^{i\theta}\alpha\rangle|0\rangle+a|e^{-i\theta}\alpha\rangle|1\rangle)/\sqrt{2}$. Projecting the qubus state into the x-quadrature eigenstate $|x\rangle$ via homodyne detection, which is the measurement we depict as $\tilde{Z}$, we obtain the conditional unnormalized state $|\psi(x)\rangle$

$$|\psi(x)\rangle=\frac{f(x,\alpha)}{\sqrt{2}}(a|0\rangle+b|1\rangle)+\frac{f(x,\alpha\cos(\theta))}{\sqrt{2}}(e^{i\phi(x)}b|0\rangle+e^{-i\phi(x)}a|1\rangle),\quad(1)$$

where

$$f(x,\beta)=\frac{1}{(2\pi)^{1/4}}\exp\left(\frac{-(x-2\beta)^2}{4}\right),\quad(2)$$

$$\phi(x)=\alpha x\sin(\theta)-\alpha^2\sin(2\theta),\quad(3)$$

since $\langle x|\alpha e^{\pm i\theta}\rangle=e^{\pm i\phi(x)}f(x,\alpha\cos(\theta))$ and $\langle x|\alpha\rangle=f(x,\alpha)$ for real α [17,18].

The weights $f(x,\alpha)$ and $f(x,\alpha\cos(\theta))$ are Gaussian functions with the same variance but different means, given by 2α and $2\alpha\cos(\theta)$, respectively. Given $x_0=\alpha[1+\cos(\theta)]$, the midpoint between $f(x,\alpha)$ and $f(x,\alpha\cos(\theta))$, one can maximize the fidelity of obtaining the desired state $a|0\rangle+b|1\rangle$ (averaged over all possible values of x) by simply doing nothing when $x>x_0$ [where $f(x,\alpha)>f(x,\alpha\cos(\theta))$], or applying $Z_{\phi(x)}=\exp[-i\phi(x)Z]$, a Pauli Z rotation by $\phi(x)$, followed by a Pauli X, when $x\leq x_0$. For simplicity, the teleportation corrections are not explicitly depicted in the circuit diagrams.

A. Average fidelities

In order to quantify the performance of the protocols just described, consider the *process fidelity* [19–21]. The process fidelity between two quantum operations is obtained by computing the state fidelity between states isomorphic to the processes under the Choi-Jamiołkowski isomorphism. The state fidelity between the density matrices ρ_1 and ρ_2, when ρ_1 is a pure state (i.e., $\rho_1=|\psi_1\rangle\langle\psi_1|$) reduces to $F(\psi_1,\rho_2)=\langle\psi_1|\rho_2|\psi_1\rangle$ [21]. In order to compare a quantum process $\mathcal{E}$ acting on a D-dimensional system to another quantum process $\mathcal{F}$ acting on the same system, we define the process fidelity as the state fidelity between the states

$$\rho_{\mathcal{E}} = \mathbb{1}_1 \otimes \mathcal{E}_2\left(\frac{1}{\sqrt{d}}\sum_{i=1}^{D}|ii\rangle_{12}\right), \tag{4}$$

$$\rho_{\mathcal{F}} = \mathbb{1}_1 \otimes \mathcal{F}_2\left(\frac{1}{\sqrt{d}}\sum_{i=1}^{D}|ii\rangle_{12}\right). \tag{5}$$

In the case of single-qubit processes, we just need to consider the action of the process on one of the qubits of the state $\frac{1}{\sqrt{2}}(|00\rangle \pm |11\rangle)$. The operational meaning of the process fidelity is given by considering the projection of the first qubit of the state in Eq. (4) into a particular state $a|0\rangle + b|1\rangle$. In this case, the second qubit collapses into the state corresponding to the output of the process acting on the state $a|0\rangle + b|1\rangle$. Thus a high state fidelity between the outputs $\rho_{\mathcal{E}}$ and $\rho_{\mathcal{F}}$, averaged over all input states $a|0\rangle + b|1\rangle$, is by definition a high process fidelity between the operations $\mathcal{E}$ and $\mathcal{F}$.

Consider the state

$$|\psi_{\pm}\rangle = \frac{1}{\sqrt{2}}(|0,\alpha\rangle \pm |1,\alpha e^{i\theta}\rangle), \tag{6}$$

produced when the circuit in Fig. 1(a) acts on one-half of the maximally entangled state $\frac{1}{\sqrt{2}}(|00\rangle \pm |11\rangle)$, and which depends on the qubit measurement outcome. As the relative phase is known, and the correction can be performed after the state is teleported back to a qubit, for each of the outcomes we can compare this state with the ideal state expected from the definition of the basis states for the qubus. Since this is the desired state corresponding to our coherent state encoding, the process fidelity is 1 for one-bit teleportation into the qubus, without any approximations.

For the case in which we teleport the state from the qubus back into the qubit, using the circuit in Fig. 1(b), we consider the action of the process on the second mode of the state $|\psi_+\rangle$ from Eq. (6). When considering Fig. 1(b) alone, this is not, strictly speaking, the Choi-Jamiołkowski isomorphism, although it does give the same operational meaning for the process fidelity as a precursor to the fidelity between the outputs of the different processes being compared, as any superposition of $\{|\alpha\rangle, |\alpha e^{i\theta}\rangle\}$ can be prepared from $|\psi_+\rangle$ by projecting the qubit into some desired state. We expect the output state to be $\frac{1}{\sqrt{2}}(|00\rangle + |11\rangle)$ from the definition of the basis states, but we instead obtain the unnormalized states

$$|\psi_E(x > x_0)\rangle = \frac{f(x,\alpha)}{\sqrt{2}}\left(\frac{|00\rangle + |11\rangle}{\sqrt{2}}\right) + \frac{f(x,\alpha\cos(\theta))}{\sqrt{2}}\left(\frac{e^{-i\phi(x)}|01\rangle + e^{i\phi(x)}|10\rangle}{\sqrt{2}}\right), \tag{7}$$

$$|\psi_E(x < x_0)\rangle = \frac{f(x,\alpha)}{\sqrt{2}}\left(\frac{e^{-i\phi(x)}|01\rangle + e^{i\phi(x)}|10\rangle}{\sqrt{2}}\right) + \frac{f(x,\alpha\cos(\theta))}{\sqrt{2}}\left(\frac{|00\rangle + |11\rangle}{\sqrt{2}}\right). \tag{8}$$

The normalized output state, averaged over all x outcomes, is

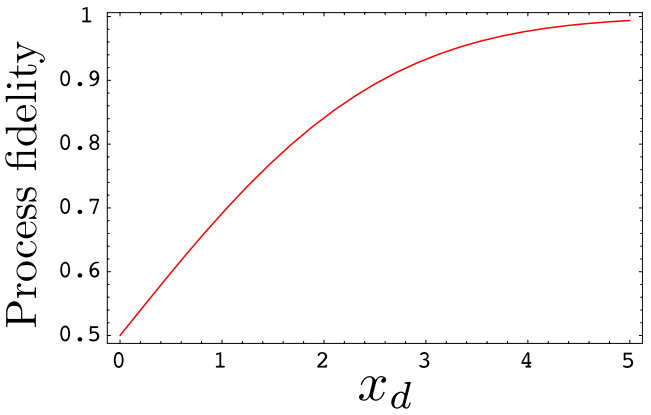

FIG. 2. (Color online) Fidelity F_p of one-bit teleportation from the qubus to a qubit, as a function of x_d.

$$\rho = \int_{x_0}^{\infty} |\psi_E(x > x_0)\rangle\langle\psi_E(x > x_0)|dx + \int_{-\infty}^{x_0} |\psi_E(x < x_0)\rangle\langle\psi_E(x < x_0)|dx, \tag{9}$$

so that the average process fidelity for one-bit teleportation into a qubit is

$$F_p = \frac{1}{2}(\langle 00| + \langle 11|)\rho(|00\rangle + |11\rangle) = \int_{x_0}^{\infty}\frac{1}{2}f^2(x,\alpha) + \int_{-\infty}^{x_0}\frac{1}{2}f^2(x,\alpha\cos(\theta)) = \frac{1}{2} + \frac{1}{2}\,\mathrm{erf}\left(\frac{x_d}{2\sqrt{2}}\right), \tag{10}$$

where $x_d = 2\alpha[1-\cos(\theta)] \approx \alpha\theta^2$ for small θ. Teleportation from the qubus into the qubit is not perfect, even in the ideal setting we consider, because the states $|\alpha\rangle$ and $|e^{i\theta}\alpha\rangle$ cannot be distinguished perfectly. However, F_p can be made arbitrarily close to 1 by letting $x_d \to \infty$, or $\alpha\theta^2 \to \infty$ if $\theta \ll 1$, as seen in Fig. 2. This corresponds to increasing the distinguishability of the coherent states $|\alpha\rangle$ and $|e^{i\theta}\alpha\rangle$.

B. Post-selected teleportation

In order to improve the average fidelity of the teleportations without changing the physical parameters α and θ of the basis states, one can post-select the outcomes of the x-quadrature measurements when teleporting states from the qubus mode to a qubit, as these outcomes essentially herald the fidelity of the output state with the desired state. Discarding the states with fidelity below a certain threshold allows for the average fidelity to be boosted, even in the case in which $\alpha\theta^2 \gg 1$, at the cost of a certain probability of failure. This is particularly useful for the preparation of quantum states which are used as resources for some quantum information processing tasks.

Instead of accepting all states corresponding to all x outcomes of the homodyne measurement that implements $\tilde{Z}$, we

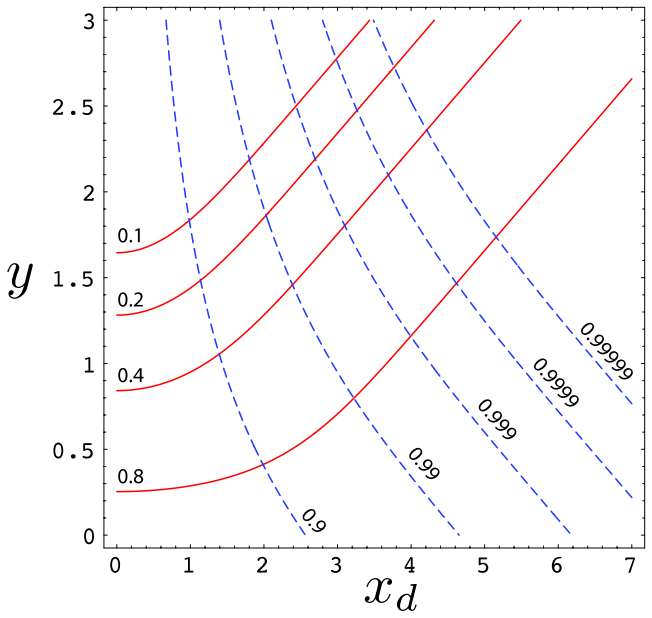

FIG. 3. (Color online) Contour lines for post-selected fidelity $F_{p,y}$ of one-bit teleportation from the qubus to a qubit (dashed blue), and success probability for post-selection (solid red), as a functions of x_d and y.

only accept states corresponding to outcomes that are far enough away from the midpoint x_0, since the state at x_0 has the lowest fidelity with the desired state. More explicitly, we only accept states corresponding to measurement outcomes that are smaller than x_0-y or larger than x_0+y. This post-selection can only be performed for one-bit teleportation from the qubus to the qubit, yielding a probability of success given by

$$\Pr(|x-x_0|>y)=\frac{1}{2}\left[\operatorname{erfc}\left(\frac{2y-x_d}{2\sqrt{2}}\right)+\operatorname{erfc}\left(\frac{2y+x_d}{2\sqrt{2}}\right)\right], \tag{11}$$

and process fidelity conditioned on the successful outcome given by

$$F_{p,y}=\frac{\operatorname{erfc}\left(\frac{2y-x_d}{2\sqrt{2}}\right)}{\operatorname{erfc}\left(\frac{2y-x_d}{2\sqrt{2}}\right)+\operatorname{erfc}\left(\frac{2y+x_d}{2\sqrt{2}}\right)}. \tag{12}$$

The effect of discarding some of the states depending on the measurement outcome for the teleportation in Fig. 1(b) is depicted in Fig. 3. In particular, we see that the process fidelity can be made arbitrarily close to 1 at the cost of lower probability of success, while α and θ are unchanged, since

$$\lim_{y\to\infty} F_{p,y}=1. \tag{13}$$

As the probability mass is highly concentrated due to the Gaussian shape of the wave packets, the probability of success drops superexponentially fast as a function of y. This is because for large z, we have [22]

$$\frac{2}{\sqrt{\pi}}\frac{e^{-z^2}}{z+\sqrt{z^2+2}}<\operatorname{erfc}(z)<\frac{2}{\sqrt{\pi}}\frac{e^{-z^2}}{z+\sqrt{z^2+\frac{4}{\pi}}}. \tag{14}$$

This fast decay corresponds to the contour lines for decreasing probability of success getting closer and closer in Fig. 3. Thus, while the fidelity can be increased arbitrarily via post-selection (by increasing y), this leads to a drop in the probability of obtaining the successful outcome for post-selection. Note that, despite this scaling, significant gains in fidelity can be obtained by post-selection while maintaining the physical resources such as α and θ fixed, and while maintaining a reasonable probability of success. In particular, if $x_d=2.5$, increasing y from 0 to 1.25 takes the fidelity from 0.9 to 0.99 while the probability of success only drops from 1 to 0.5.

If the probability of success is to be maintained constant, a linear increase in x_d can bring the fidelity exponentially closer to unity, as is evident in Fig. 3. As x_d is proportional to the amplitude α of the coherence state, this can be achieved while maintaining θ constant. Since θ is usually the parameter that is hard to increase in an experimental setting, this is highly advantageous.

Instead of discarding the outputs with unacceptable fidelity, one can also use the information that the failure is heralded to recover and continue the computation. In the case of the one-bit teleportations described here, such an approach would require active quantum error correction or quantum erasure codes—the type of codes necessary for heralded errors—which have much higher thresholds than general quantum-error correcting codes [9]. We will not discuss such a possibility further in this paper, and will focus instead on post-selection for quantum gate construction and state preparation.

III. UNIVERSAL COMPUTATION WITH QUBUS LOGIC

Previous work by Ralph *et al.* [23,24] and Gilchrist *et al.* [25] illustrated the construction of a universal quantum computer using what we call *coherent state logic*. In these schemes, a universal set of gates is applied to qubit basis states defined as $|0\rangle_L=|-\alpha'\rangle$ and $|1\rangle_L=|\alpha'\rangle$, using partial Bell state measurements and cat states of the form $(|-\alpha'\rangle+|\alpha'\rangle)/\sqrt{2}$ as resources. To perform a universal set of gates, a total of 16 ancilla cat states are necessary [24]. For $\alpha'\geqslant 2$, the qubits $|-\alpha'\rangle$ and $|\alpha'\rangle$ are approximately orthogonal since $|\langle\alpha'|-\alpha'\rangle|^2=e^{-4\alpha'^2}\leqslant 10^{-6}$.

Using the one-bit teleportations in Fig. 1, we can also perform a universal set of gates on a Hilbert space spanned by the states $|\mathbf{0}\rangle_L=|\alpha\rangle$ and $|\mathbf{1}\rangle_L=|e^{\pm i\theta}\alpha\rangle$, which we call *qubus logic*. As mentioned in the previous section, the two states defined for the logical $|\mathbf{1}\rangle_L$ are indistinguishable when we homodyne detect along the x-quadrature, a fact that will become important later. The overlap between these basis states $|\langle\alpha|e^{\pm i\theta}\alpha\rangle|^2=e^{-2|\alpha|^2(\cos\theta-1)}\approx e^{-|\alpha|^2\theta^2}$ (for small θ) is close to 0 provided $\alpha\theta\gg 1$, so that we may consider them orthogonal; e.g., for $\alpha\theta>3.4$, we have $|\langle\alpha|e^{i\theta}\alpha\rangle|^2\leqslant 10^{-6}$. It can be seen that our basis states are equivalent to the basis states of co-

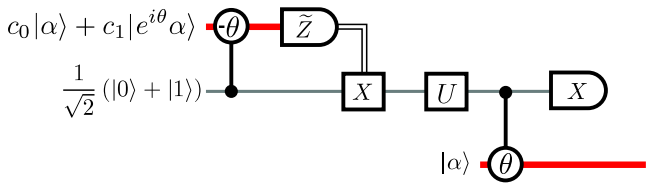

FIG. 4. (Color online) A single-qubit gate performed on $c_0|\alpha\rangle + c_1|e^{i\theta}\alpha\rangle$.

herent state logic given a displacement and a phase shifter. That is, if we displace the arbitrary state $a|\alpha\rangle + b|\alpha e^{i\theta}\rangle$ by $D[-\alpha\cos(\theta/2)e^{i\theta/2}]$ and apply the phase shifter $e^{i(\pi-\theta)\hat{n}/2}$, we have $a|\alpha\sin(\theta/2)\rangle + be^{i\alpha^2\sin(\theta)/2}|-\alpha\sin(\theta/2)\rangle$. If we now set $\alpha' = \alpha\sin(\theta/2) \approx \alpha\theta/2$, for small θ, we see that our arbitrary qubus logical state is equivalent to an arbitrary coherent state qubit. The $e^{i\alpha^2\sin(\theta)/2}$ phase factor can be corrected once we use a single-bit teleportation. If $\alpha' \geqslant 2$, then $\alpha\theta \geqslant 4$, which is already satisfied by the approximate orthogonality condition $\alpha\theta \gg 1$. It is important to note that, although the basis states are equivalent, the gate constructions we describe for qubus logic are very different from the gate constructions for coherent state logic.

We compare qubus logic and coherent state logic based on resource usage, i.e., the number of ancilla states and controlled rotations necessary to perform each operation. Since the cat state ancillas needed in coherent state logic, $(|-\alpha'\rangle + |\alpha'\rangle)/\sqrt{2}$, can be made using the circuit in Fig. 1(a) with an incident photon in the state $(|0\rangle + |1\rangle)/\sqrt{2}$ provided $\alpha' = \alpha\sqrt{[1-\cos(\theta)]/2} \approx \alpha\theta/2$, we consider the 16 ancilla cat states required in [24] for a universal set of gates to be equivalent to 16 controlled rotations.

In the next two sections, we describe how to construct arbitrarily good approximations to any single-qubit unitary rotation as well as the unitary CSIGN=diag(1,1,1,−1) in qubus logic, as this is sufficient for universal quantum computation [26].

A. Single-qubit gates

An arbitrary single-qubit unitary gate U can be applied to the state $c_0|\alpha\rangle + c_1|e^{i\theta}\alpha\rangle$ by the circuit shown in Fig. 4. We first teleport this state to the qubit using the circuit in Fig. 1(b) and then perform the desired unitary U on the qubit, giving $U(c_0|0\rangle + c_1|1\rangle)$. We can teleport this state back to the qubus mode with Fig. 1(a), while the $\tilde{Z}$ correction can be delayed until the next single-qubit gate, where it can be implemented by applying a Z in addition to the desired unitary. If it happens that this single-qubit rotation is the last step of an algorithm, we know that this $\tilde{Z}$ error will not effect the outcome of a homodyne measurement (which is equivalent to a measurement in the Pauli Z eigenbasis), so that this correction may be ignored. In total, this process requires two controlled rotations.

Since arbitrary single-qubit gates are implemented directly in the two-level system, the only degradation in the performance comes from the teleportation of the state from the qubus to the qubit, resulting in the fidelity given in Eq. (10).

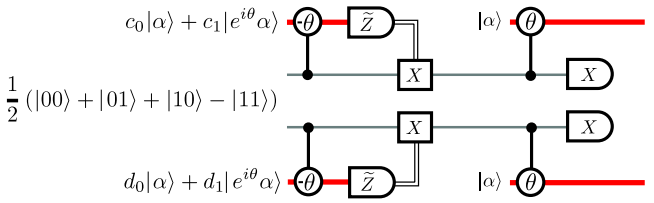

FIG. 5. (Color online) Circuit used to perform a CSIGN between states in qubus logic.

In the case in which we wish to perform a bit flip on the qubit $c_0|\alpha\rangle + c_1|e^{i\theta}\alpha\rangle$, we can simply apply the phase shifter $e^{-i\theta\hat{n}}$ to obtain $c_0|e^{-i\theta}\alpha\rangle + c_1|\alpha\rangle$, similarly to the bit flip gate in [24].

Post-selected implementation of single-qubit gates

The fidelity of single-qubit gates in qubus logic can be improved simply by using post-selected teleportations. For simplicity, if we disregard the second one-bit teleportation, which transfers the state back to qubus logic, we obtain the probability of success given in Eq. (11) and the conditional process fidelity given in Eq. (12).

B. Two-qubit gates

To implement the entangling CSIGN gate, we teleport our qubus logical state onto the polarization entangled state $\frac{1}{2}(|00\rangle + |01\rangle + |10\rangle - |11\rangle)$. The state $\frac{1}{2}(|00\rangle + |01\rangle + |10\rangle - |11\rangle) = (1 \otimes H)(|00\rangle + |11\rangle)/\sqrt{2}$, where H represents a Hadamard gate, can be produced offline by any method that generates a maximally entangled pair of qubits. As described previously in the context of error correction, such a state can be produced with controlled rotations [5]. If we start with the qubus coherent state $|\sqrt{2}\alpha\rangle$ and an eigenstate of the Pauli X operator $(|0\rangle + |1\rangle)/\sqrt{2}$ incident on Fig. 1(a), we obtain $|\sqrt{2}\alpha\rangle + |\sqrt{2}e^{i\theta}\alpha\rangle$. Next we put this through a symmetric beam splitter to obtain $\frac{1}{\sqrt{2}}(|\alpha,\alpha\rangle + |e^{i\theta}\alpha, e^{i\theta}\alpha\rangle)$ [25]. If we now teleport this state to polarization logic with Fig. 1(b), we have, to a good approximation, the Bell state $(|00\rangle + |11\rangle)/\sqrt{2}$, and with a local Hadamard gate we finally obtain $\frac{1}{2}(|00\rangle + |01\rangle + |10\rangle - |11\rangle)$. To make this state, we have used three controlled rotations and one ancilla photon. Since we are only concerned with preparing a resource state that in principle can be stored, we can perform post-selection at the teleportations to ensure the state preparation is of high fidelity, as described in Sec. II B.

After this gate teleportation onto qubits, we teleport back to the qubus modes after a possible X correction operation. The overall circuit is shown in Fig. 5. This CSIGN gate requires four controlled rotations. As with the single-qubit gates, $\tilde{Z}$ corrections may be necessary after the final teleportations of Fig. 5, but these corrections can also be delayed until the next single-qubit gate.

We can see what affect the condition $\alpha\theta^2 \gg 1$ has on the function of the gate in Fig. 5 by looking at the process fidelity. As this gate operates on two qubits, the input state to the process we want to compare is

$$\frac{1}{2}(|0,0\rangle|\alpha,\alpha\rangle + |0,1\rangle|\alpha,\alpha e^{i\theta}\rangle + |1,0\rangle|\alpha e^{i\theta},\alpha\rangle + |1,1\rangle|\alpha e^{i\theta},\alpha e^{i\theta}\rangle). \quad (15)$$

From the basis states we have defined, we expect the output

$$|\psi_2\rangle = \frac{1}{2}(|0,0\rangle|\alpha,\alpha\rangle + |0,1\rangle|\alpha,\alpha e^{i\theta}\rangle + |1,0\rangle|\alpha e^{i\theta},\alpha\rangle - |1,1\rangle|\alpha e^{i\theta},\alpha e^{i\theta}\rangle). \quad (16)$$

The unnormalized state output from Fig. 5 is

$$\begin{aligned}|\psi_{2,o}\rangle = \frac{1}{4}\{&f(x,\alpha)f(x',\alpha)[|00\rangle|00\rangle + |01\rangle|01\rangle + |10\rangle|10\rangle \\ &- |11\rangle|11\rangle] + f(x,\alpha)f(x',\alpha\cos(\theta))[e^{-i\phi(x')}(|00\rangle|01\rangle \\ &+ |10\rangle|11\rangle) + e^{i\phi(x')}(|01\rangle|00\rangle - |11\rangle|10\rangle)] \\ &+ f(x,\alpha\cos(\theta))f(x',\alpha)[e^{-i\phi(x)}(|00\rangle|10\rangle + |01\rangle|11\rangle) \\ &+ e^{i\phi(x)}(|10\rangle|00\rangle - |11\rangle|01\rangle)] \\ &+ f(x,\alpha\cos(\theta))f(x',\alpha\cos(\theta))[e^{-i[\phi(x)+\phi(x')]}|00\rangle|11\rangle \\ &+ e^{i(\phi(x')-\phi(x))}|01\rangle|10\rangle + e^{i[\phi(x)-\phi(x')]}|10\rangle|01\rangle \\ &- e^{i[\phi(x)+\phi(x')]}|11\rangle|00\rangle]\}, \end{aligned} \quad (17)$$

where x and x' are the outcomes of the $\tilde{Z}$ measurements (top and bottom in Fig. 5, respectively). For simplicity, we disregard the final teleportations back to qubus modes, as we have already discussed how they affect the average fidelity of the state in Sec. II. Since we have two homodyne measurements to consider, we need to look at the four cases: (i) x greater than x_0 and x' greater than x_0; (ii) x greater than x_0 and x' less than x_0; (iii) x greater than x_0 and x' less than x_0; (iv) x less than x_0 and x' less than x_0. The necessary corrections for each of these cases are (i) $\mathbb{1}\otimes\mathbb{1}$, (ii) $\mathbb{1}\otimes Z_{\phi(x')}X$, (iii) $Z_{\phi(x)}X\otimes\mathbb{1}$, and (iv) $Z_{\phi(x)}X\otimes Z_{\phi(x')}X$. Integrating over x and x' for these four different regions, one finds the process fidelity to be

$$F_{\text{CSIGN}} = \frac{1}{4}\left[1 + \text{erf}\left(\frac{x_d}{2\sqrt{2}}\right)\right]^2, \quad (18)$$

which just corresponds to the square of the process fidelity for a one-bit teleportation into qubits, as the only source of failure is the indistinguishability of the basis states for qubus logic. A plot showing how this fidelity scales as a function of x_d is shown in Fig. 6.

Post-selected implementation of the entangling gate

We can counteract the reduction in fidelity shown in Fig. 6 in a similar way to the single-qubit gate case, by only accepting measurement outcomes less than x_0-y and greater than x_0+y. We find the success probability and conditional fidelity to be

$$P_{\text{CSIGN}} = \frac{1}{4}\left[\text{erfc}\left(\frac{2y-x_d}{2\sqrt{2}}\right) + \text{erfc}\left(\frac{2y+x_d}{2\sqrt{2}}\right)\right]^2, \quad (19)$$

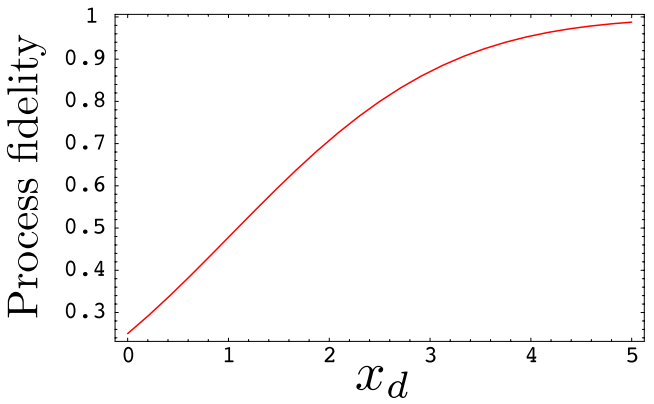

FIG. 6. (Color online) Fidelity F_{CSIGN} of one-bit CSIGN teleportation from the qubus to a qubit, as a function of x_d.

$$F_{\text{CSIGN},y} = \left(\frac{\text{erfc}\left(\frac{2y-x_d}{2\sqrt{2}}\right)}{\text{erfc}\left(\frac{2y-x_d}{2\sqrt{2}}\right) + \text{erfc}\left(\frac{2y+x_d}{2\sqrt{2}}\right)}\right)^2, \quad (20)$$

respectively. As before, we see that the process fidelity can be made arbitrarily close to 1 at the cost of lower probability of success. It should also be immediately clear that as $y \to 0$, we have $P_{\text{CSIGN}} \to 1$ and $F_{\text{CSIGN},y} \to F_{\text{CSIGN}}$.

We see the effect of ignoring some of the homodyne measurements in Fig. 7. Even though performance is degraded because of the use of two one-bit teleportations, the general scalings of the fidelity and probability of success with respect to y and x_d are similar to the one-bit teleportation. In

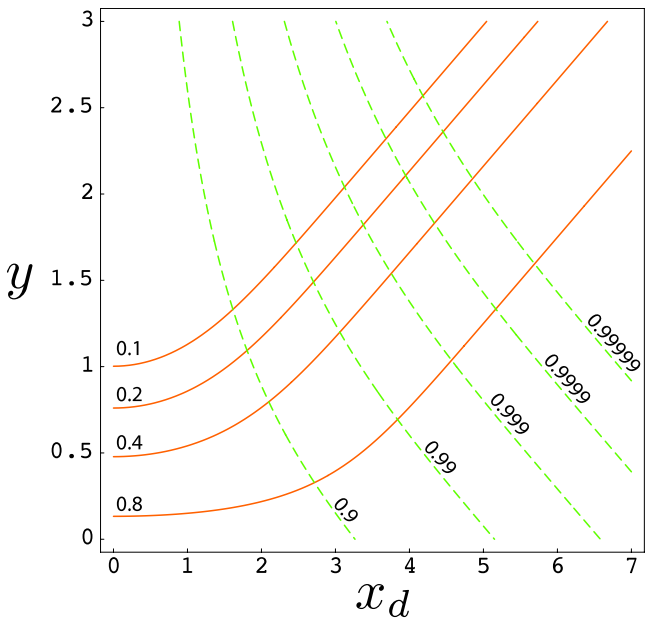

FIG. 7. (Color online) Contour lines for post-selected fidelity $F_{\text{CSIGN},y}$ of CSIGN teleportation from the qubus to a qubit (dashed green), and success probability for post-selection (solid gold), as functions of x_d and y.

particular, we see that the fidelity can be increased significantly by increasing x_d (or equivalently, α).

C. Comparison between qubus logic and coherent state logic

The total number of controlled rotations necessary to construct our universal set of quantum gates on qubus logic, consisting of an arbitrary single-qubit rotation and a CSIGN gate, is nine—the construction of an arbitrary single-qubit gate required two controlled rotations and the construction of a CSIGN gate required seven, three for the entanglement production and four for the gate operation. This is in contrast to the 16 controlled rotations (where we assume each controlled rotation is equivalent to a cat state ancilla) necessary for a universal set of gates in coherent state logic [23–25], where an arbitrary single-qubit rotation is constructed via $\exp(-i\frac{\vartheta}{2}Z)\exp(-i\frac{\pi}{4}X)\exp(-i\frac{\varphi}{2}Z)\exp(i\frac{\pi}{4}X)$, with each rotation requiring two cat state ancilla, and a CNOT gate requiring eight cat state ancilla.

As a further comparison, we compare the resource consumption of the qubus logic scheme with the recent extension to the coherent state logic scheme by Lund *et al.* [27] that considers small-amplitude coherent states. In this scheme, gate construction is via unambiguous gate teleportation, where the failure rate for each teleportation is dependent on the size of the amplitude of the coherent state logical states. Each gate teleportation requires offline probabilistic entanglement generation. On average, an arbitrary rotation about the Z axis would require three cat state ancilla and both the Hadamard and CSIGN gate would each require 27 cat state ancilla.

The scheme proposed here yields significant savings compared to previous schemes in terms of the number of controlled rotations necessary to apply a universal set of gates on coherent states. These savings are for operations on physical, unencoded qubits. A full analysis of resources for encoded operations for some error model may lead to a reduction in resources compared to Lund *et al.* [27], however this is an open question.

It should be noted that in an experimental setting, the construction of one type of resource, either controlled rotations on a quantum bus or cat state ancilla, may be easier than the other. In such a case, the resource consumption mentioned here may require alterations.

IV. CONSTRUCTION OF CLUSTER STATES

As we have pointed out in the previous section, the GHZ preparation scheme used for fault-tolerant error correction with strong coherent beams [5] can be used to perform CSIGN gate teleportation. This approach can be generalized to aid in the construction of cluster states [6], as GHZ states are locally equivalent to star graph states [28,29]. Once we have GHZ states, we can either use CNOT gates built with the aid of a qubus [30,31] to deterministically join them to make a large cluster state, or use fusion gates [8] to join them probabilistically.

Recent work by Jin *et al.* [32] showed a scheme to produce arbitrarily large cluster states with a single coherent probe beam. In this scheme, N copies of the state $(|H\rangle+|V\rangle)/\sqrt{2}$ can be converted into the GHZ state $(|H\rangle^{\otimes N}+|V\rangle^{\otimes N})/\sqrt{2}$ with the use of N controlled rotations and a single homodyne detection. However, the size of the controlled rotations necessary scales exponentially with the size of the desired GHZ state–the Nth controlled rotation would need to be $2^{N-1}-1$ times larger than the first controlled rotation applied to the probe beam. For example, if we consider an optimistic controlled rotation θ of order 0.1, once N reaches 10 we would require a controlled rotation on the order of π, which is infeasible for most physical implementations. In the next section, we describe how to prepare GHZ states that only require large-amplitude coherent states while using the same fixed controlled rotations θ and $-\theta$.

A. GHZ state preparation and repetition encoding

We mentioned a scheme in the previous section to construct the Bell state $|00\rangle+|11\rangle$, but this can be generalized to prepare GHZ states of any number of subsystems. We first start with the state $(|0\rangle+|1\rangle)/\sqrt{2}$ and teleport it to a qubus initially in the larger amplitude $|\sqrt{N}\alpha\rangle$. This will give $(|\sqrt{N}\alpha\rangle+|\sqrt{N}\alpha e^{i\theta}\rangle)/\sqrt{2}$. Sending this state through an N port beam splitter with $N-1$ vacuum states in the other ports gives $(|\alpha\rangle^{\otimes N}+|\alpha e^{i\theta}\rangle^{\otimes N})/\sqrt{2}$. Each of these modes can then be teleported back to qubits, yielding $(|0\rangle^{\otimes N}+|1\rangle^{\otimes N})/\sqrt{2}$. The resources that we use to make a GHZ state of size N are $N+1$ controlled rotations, $N+1$ single-qubit ancillas, a single-qubit measurement, and N homodyne detections.

This circuit can also function as an encoder for a quantum repetition code, in which case we can allow any input qubit state $a|0\rangle+b|1\rangle$ and obtain an approximation to $a|0\rangle^{\otimes N}+b|1\rangle^{\otimes N}$. In order to evaluate the performance of this process, we once again calculate the process fidelity by using the input state $\frac{1}{\sqrt{2}}(|00\rangle+|11\rangle)$ and acting on the second subsystem. Using a generalization of Eq. (17), we calculate the effect of $\alpha\theta^2 \gg 1$ on the production of a GHZ state of size N to be

$$F_{\mathrm{REP}} = \frac{1}{2^N}\left[1+\mathrm{erf}\left(\frac{x_d}{2\sqrt{2}}\right)\right]^N. \tag{21}$$

Again, this corresponds to the process fidelity of a single one-bit teleportation into a qubit raised to the Nth power. The fidelity of preparing repetition encoded states drops exponentially in N. In Fig. 8, we show the fidelity as a function of x_d for $N=3$ and for $N=9$.

B. Post-selected implementation of GHZ state preparation and repetition encoding

The reduction in fidelity due to $\alpha\theta^2 \gg 1$ in Eq. (21) can be counteracted, as before, by simply performing post-selection during the one-bit teleportations into the qubits.

We find the success probability and conditional fidelity to be

$$P_{\mathrm{REP}} = \frac{1}{2^N}\left[\mathrm{erfc}\left(\frac{2y-x_d}{2\sqrt{2}}\right)+\mathrm{erfc}\left(\frac{2y+x_d}{2\sqrt{2}}\right)\right]^N, \tag{22}$$

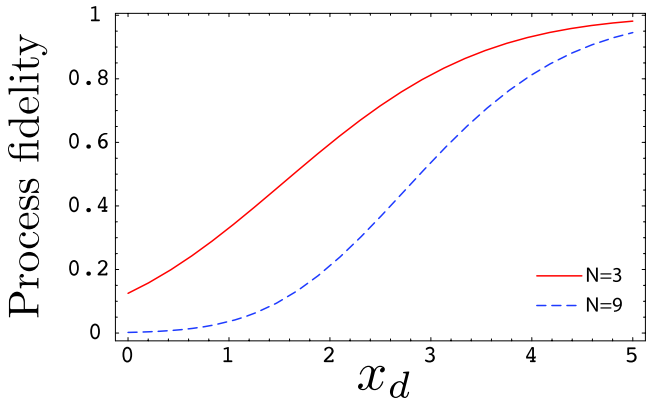

FIG. 8. (Color online) Process fidelity F_{REP} of repetition encoding as a function of x_d.

$$F_{\mathrm{REP},y} = \left(\frac{\mathrm{erfc}\left(\frac{2y - x_d}{2\sqrt{2}} \right)}{\mathrm{erfc}\left(\frac{2y - x_d}{2\sqrt{2}} \right) + \mathrm{erfc}\left(\frac{2y + x_d}{2\sqrt{2}} \right)} \right)^N . \quad (23)$$

As $y \to 0$, we see that $P_{\mathrm{REP}} \to 1$ and $F_{\mathrm{REP},y} \to F_{\mathrm{REP}}$.

The effect of discarding some of the states corresponding to undesired homodyne measurement outcomes can be seen in Figs. 9 and 10. Thus, as discussed in Sec. II B, one can prepare a state encoded in the repetition code with an arbitrarily high process fidelity, regardless of what θ and α are. The expected degradation in performance due to the additional teleportations is also evident in the faster decay of the probability of success with larger y.

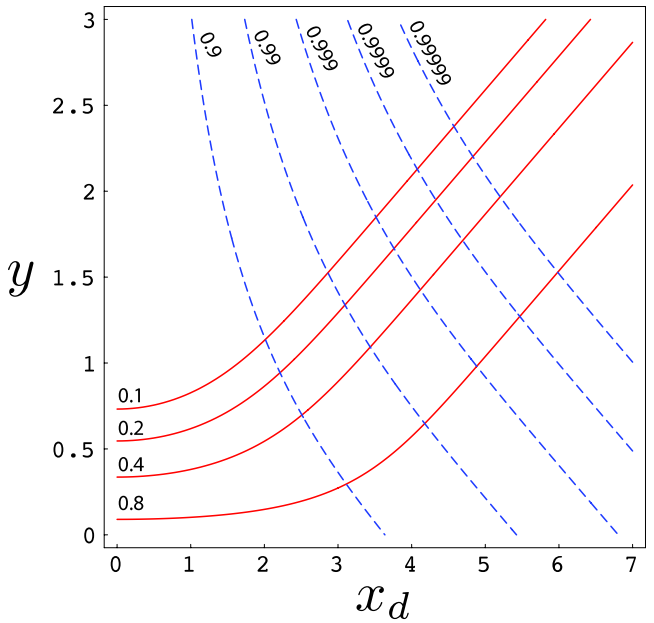

FIG. 9. (Color online) Contour lines for post-selected process fidelity $F_{\mathrm{REP},y}$ of threefold repetition encoding (dashed blue), and success probability for post-selection (solid red), as functions of $\alpha\theta^2$ and y.

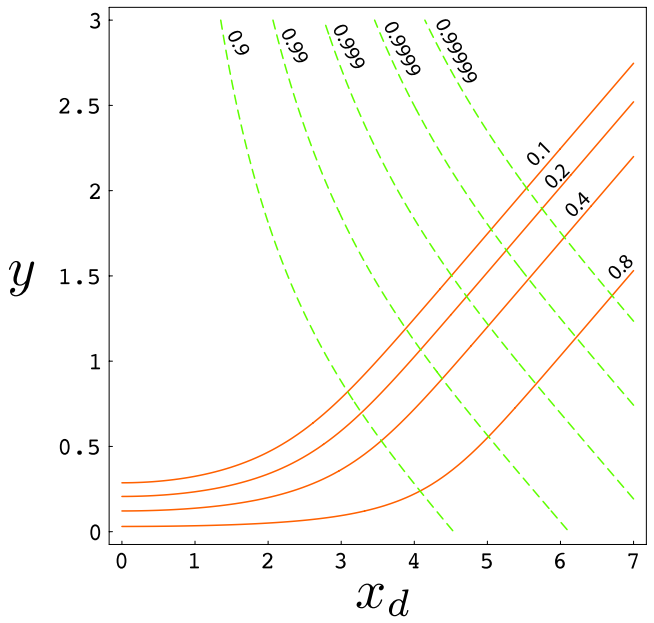

FIG. 10. (Color online) Contour lines for post-selected process fidelity $F_{\mathrm{REP},y}$ of ninefold repetition encoding (dashed green), and success probability for post-selection (solid gold), as functions of $\alpha\theta^2$ and y.

V. DISCUSSION

We have described in detail various uses for one-bit teleportations between a qubit and a qubus. Using these teleportations, we proposed a scheme for universal quantum computation, called qubus logic, which, when the number of controlled rotations is used as a measurement of resources, is a significant improvement over other proposals for quantum computation using coherent states. This scheme uses fewer interactions to perform the gates, and also allows for the use of post-selection to arbitrarily increase the fidelity of the gates given any interaction strength at the cost of lower success probabilities. Whether this scheme leads to a resource reduction when encoded operations are considered is an open question and will be the subject of a future paper.

The one-bit teleportations also allow for the preparation of highly entangled N party states known as GHZ states, which can be used in the preparation of cluster states. Moreover, the same circuitry can be used to encode states in the repetition code, which is a building block for Shor's nine-qubit code. In this case, in which we are interested in preparing resource states, the power and flexibility of post-selected teleportations can be fully exploited, as the achievable fidelity of the state preparation is independent of the interaction strength available.

The main property of the qubus which is exploited in the schemes described here is the fact that entanglement can be easily created in the qubus through the use of a beam splitter. Local operations, on the other hand, are easier to perform on a qubit. The controlled rotations allow for information to be transferred from one system to the other, allowing for the advantages of each physical system to be exploited to maximal advantage.

The fidelity suffers as the operations become more complex, as can be seen in Figs. 11 and 12. This is because

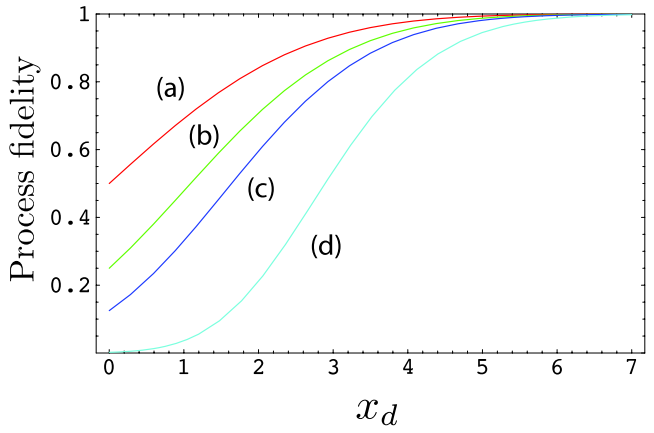

FIG. 11. (Color online) Process fidelity as a function of x_d for (a) the qubus logic single-qubit gate (F_p); (b) the CSIGN teleportation (F_{CSIGN}); (c) repetition encoding with $N=3$ (F_{REP}); (d) repetition encoding with $N=9$ (F_{REP}).

multiple uses of the imperfect one-bit teleportation from qubus to qubit are used. As the process fidelity is less than perfect, error correction would have to be used for scalable computation. However, as we have discussed, the fact that the homodyne measurements essentially herald the fidelity of the operations, it is possible to use post-selection in conjunction with error heralding to optimize the use of physical resources.

While the scheme presented has been abstracted from particular physical implementations, any physical realizations of a qubit and a continuous variable mode would suffice. The only requirements are controlled rotations, along with fast single-qubit gates and homodyne detection, which are necessary to enable feed-forward of results for the implementation of the relevant corrections.

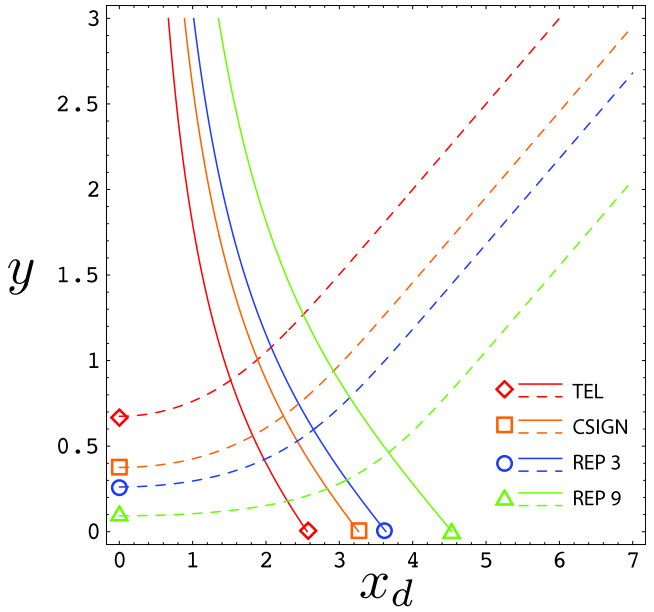

FIG. 12. (Color online) Contour plot showing the conditional process fidelity (solid curves) as a function of x_d and y for $F=0.9$ for qubus to qubit one-bit teleportation (red), CSIGN teleportation (gold), repetition encoding for $N=3$ (blue), and repetition encoding for $N=9$ (green). The dashed curves are contour curves for the probability of success for post-selection with $\Pr(|x-x_0|>y)=0.5$.

ACKNOWLEDGMENTS

We would like to thank T. C. Ralph, K. Nemoto, and W. J. Munro for valuable discussions. We are supported in part by NSERC, ARO, CIAR, MITACS, and MEXT in Japan. C.R.M. would like to thank Mike and Ophelia Lazaridis for financial support. M.S. would like to thank the Bell family for financial support.

[1] C. H. Bennett, G. Brassard, C. Crepeau, R. Jozsa, A. Peres, and W. K. Wootters, Phys. Rev. Lett. **70**, 1895 (1993).
[2] D. Gottesman and I. L. Chuang, Nature **402**, 390 (1999).
[3] E. Knill, R. Laflamme, and G. J. Milburn, Nature **409**, 46 (2001).
[4] X. Zhou, D. W. Leung, and I. L. Chuang, Phys. Rev. A **62**, 052316 (2000).
[5] C. R. Myers, M. Silva, K. Nemoto, and W. J. Munro, Phys. Rev. A **76**, 012303 (2007).
[6] R. Raussendorf and H. J. Briegel, Phys. Rev. Lett. **86**, 5188 (2001).
[7] M. A. Nielsen, Phys. Rev. Lett. **93**, 040503 (2004).
[8] D. E. Browne and T. Rudolph, Phys. Rev. Lett. **95**, 010501 (2005).
[9] E. Knill, Phys. Rev. A **71**, 042322 (2005); Nature **434**, 39 (2005).
[10] M. Silva, V. Danos, E. Kashefi, and H. Olivier, New J. Phys. **9**, 192 (2007).
[11] S. G. R. Louis, W. J. Munro, T. P. Spiller, and K. Nemoto, Phys. Rev. A **78**, 022326 (2008).
[12] H. Schmidt and A. Imamoglu, Opt. Lett. **21**, 1936 (1996).
[13] D. A. Braje, V. Balic, G. Y. Yin, and S. E. Harris, Phys. Rev. A **68**, 041801(R) (2003).
[14] Q. A. Turchette, C. J. Hood, W. Lange, H. Mabuchi, and H. J. Kimble, Phys. Rev. Lett. **75**, 4710 (1995).
[15] P. Grangier, J. A. Levenson, and J.-P. Poizat, Nature **396**, 537 (1998).
[16] D. I. Schuster *et al.*, Nature **445**, 515 (2007).
[17] C. W. Gardiner and P. Zoller, *Quantum Noise* (Springer-Verlag, Berlin, 2004).
[18] S. D. Barrett, P. Kok, K. Nemoto, R. G. Beausoleil, W. J. Munro, and T. P. Spiller, Phys. Rev. A **71**, 060302(R) (2005).
[19] A. Jamiołkowski, Rep. Math. Phys. **3**, 275 (1972).
[20] M. Horodecki, P. Horodecki, and R. Horodecki, Phys. Rev. A **60**, 1888 (1999).
[21] A. Gilchrist, N. K. Langford, and M. A. Nielsen, Phys. Rev. A **71**, 062310 (2005).
[22] E. W. Weisstein, "Erfc." From MathWorld–A Wolfram Web Resource. http://mathworld.wolfram.com/Erfc.html.
[23] T. C. Ralph, W. J. Munro, and G. J. Milburn, Proc. SPIE **4917**, 1 (2002).
[24] T. C. Ralph, A. Gilchrist, G. J. Milburn, W. J. Munro, and S.

Glancy, Phys. Rev. A **68**, 042319 (2003).
[25] A. Gilchrist, K. Nemoto, W. J. Munro, T. C. Ralph, S. Glancy, S. L. Braunstein, and G. J. Milburn, J. Opt. B: Quantum Semiclassical Opt. **6**, S828 (2004).
[26] D. P. DiVincenzo, Phys. Rev. A **51**, 1015 (1995).
[27] A. P. Lund, T. C. Ralph, and H. L. Haselgrove, Phys. Rev. Lett. **100**, 030503 (2008).
[28] M. Hein, W. Dur, J. Eisert, R. Raussendorf, M. Van den Nest, and H.-J. Briegel, e-print arXiv:quant-ph/0602096.
[29] E. T. Campbell, J. Fitzsimons, S. C. Benjamin, and P. Kok, e-print arXiv:quant-ph/0702209.
[30] W. J. Munro, K. Nemoto, and T. P. Spiller, New J. Phys. **7**, 137 (2005).
[31] K. Nemoto and W. J. Munro, Phys. Rev. Lett. **93**, 250502 (2004).
[32] G.-S. Jin, Y. Lin, and B. Wu, Phys. Rev. A **75**, 054302 (2007).